2013년도 2월
석사학위논문

Regulation of the Morphogenesis and Development by RapGAP9 in *Dictyostelium*

조 선 대 학 교 대 학 원

생 물 학 과

문 혜 민

Regulation of the Morphogenesis and Development by RapGAP9 in *Dictyostelium*

RapGAP9에 의한 *Dictyostelium* 세포에서 형태형성과 발달 조절

2013 년 2 월 25 일

조 선 대 학 교 대 학 원

생 물 학 과

문 혜 민

Regulation of the Morphogenesis and Development by RapGAP9 in *Dictyostelium*

지도교수 전택중

이 논문을 이학석사학위 신청 논문으로 제출함

2012 년 10월

조 선 대 학 교 대 학 원

생 물 학 과

문 혜 민

문혜민의 석사학위논문을 인준함

위원장 조선대학교 교 수 김 영 곤 (인) 

위 원 조선대학교 조교수 이 준 식 (인) 

위 원 조선대학교 조교수 전 택 중 (인) 

2012년 11월

조 선 대 학 교 대 학 원

CONTENTS

LIST OF FIGURES

LIST OF TABLE

ABBREVIATIONS

cAMP	cyclic adenosine monophosphate
cAR	cyclic AMP receptors
DAPI	4',6'-diamidine-2'-phenylindole dihydrochloride
GAP	GTPase activating proteins
GDP	Guanosine diphosphate
GEF	Guanine nucleotide exchange factor
GFP	Green fluorescent protein
GPCR	G-protein coupled receptor
GTP	Guanosine triphosphate
rRNA	ribosomal RNA

ABSTRACT

Regulation of the Morphogenesis and Development by RapGAP9 in *Dictyostelium*

Hyemin Mun

Advisor : Assistant Prof. Taeck Joong Jeon, Ph.D.

Department of Biology,

Graduate School of Chosun University

The small GTPase Rap1 is involved in the control of diverse cellular processes including integrin-mediated cell adhesion, cadherin-based cell-cell adhesion, cell polarity formation, and cell migration. Recent reports have demonstrated that the importance of Rap1-specific GTPase-activating proteins (GAPs) in the spatial and temporal regulation of Rap1 activity during cell migration and development in *Dictyostelium*. Here, I identified another Rap1 GAP-domain containing protein by bioinformatic search of *Dictyostelium* database (www.dictybase.org). The putative Rap1 GAP domain of RapGAP9 showed high sequence homologies with those of

human Rap1GAP and *Dictyostelium* RapGAP3. To investigate the functions of RapGAP9, I prepared *rapGAP9* null cells by homologous recombination and found that *rapGAP9* null cells were more flattened and spread than wild-type cells. *rapGAP9* null cells displayed a small increase of cell-substratum attachment compared with wild-type cells. The loss of RapGAP9 resulted in an altered morphology of fruiting body with a shorter length of stalk and spore. These data suggest that RapGAP9 is involved in cell adhesion and multicellular development. The localization assay showed that RapGAP9 localized to the cell cortex and preferentially at the leading edge in migrating cells. Upon chemoattractant stimulation, RapGAP9 was translocated transiently and rapidly to the cell cortex from the cytosol. Rap1 is emerging as a major regulator of cytoskeleton reorganization and cell adhesion in *Dictyostelium*. Identification and characterization of RapGAP9 in this study will provide further insight into the molecular mechanism by which Rap1 regulates cytoskeleton reorganization and morphogenesis in *Dictyostelium*.

국문초록

RapGAP9에 의한 *Dictyostelium* 세포의 형태형성과 발달 조절

Small GTPase Rap1 은 integrin-매개 세포부착, cadherin-기반 세포-세포간 부착, 세포 극성 형성, 그리고 세포 이동의 조절에 관여한다. 최근의 연구에 의하면 *Dictyostelium* 세포에서 세포 이동과 발달 동안 Rap1의 시공간적인 조절에서 Rap1-특이 GTPase-활성 단백질 (GAPs)의 중요성을 입증하였다. 본 연구에서는 *Dictyostelium* database에서 생물정보학적 검색에 의한 또 다른Rap1-GAP-도메인을 포함한 단백질을 찾아냈고, 임의적으로 RapGAP9이라 이름하였다. RapGAP9의 잠정적인 Rap1GAP 도메인은 human Rap1GAP1과 *Dictyostelium* RapGAP3의 도메인과 서열이 매우 일치하는 것을 보인다. RapGAP9의 기능을 입증하기 위해서, 상동재조합에 의해 RapGAP9이 없는 세포를 만들고 RapGAP9이 적절한 발달과 형태 형성 과정에 필요하다는 것을 발견하였다. RapGAP9이 없는 세포는 변화된 형태의 과실체로 대체됨을 알 수 있다. 생장단계에서는 RapGAP9이 없는 세포는 야생종에 비해 더 납작해지고 편평해지며 세포-바닥간의 부착이 증가하고 위족의 수가 많아짐을 보인다. 이러한 결과는 RapGAP9이 세포부착과 다세포성

발달에 관련이 있음을 시사해준다. 위치조사는 RapGAP9이 세포피질에 위치하며 이동하는 세포에서는 세포 앞쪽의 돌출부위에 위치함을 보였다. 일정한 주화성 인자의 자극 동안에는, RapGAP9은 세포기질에서부터 세포피질로 일시적이고 빠르게 이동한다. RapGAP9이 cell cortex에 위치하기 위해서는 Full length construct가 필요하며, F-actin과 PI3K signaling pathway에 의존적으로 세포 피질로 이동한다. 본 연구는 Rap1에 특이적으로 비활성을 가질 것이라 추정되는 단백질인 RapGAP9에 대해 진행 하였다. Rap1은 *Dictyostelium* 세포에서 세포골격의 재배치와 세포 부착에 중요한 조절자로 밝혀져 있다. 본 연구에서 밝혀낸 RapGAP9은 *Dictyostelium* 세포에서 세포골격 재배치와 형태형성을 조절하는 Rap1의 분자상의 기작에 대한 이해를 제공할 수 있다.

I. Introduction

Chemotaxis is involved in many diverse physiological processes including the recruitment of leukocytes to the sites of infection, tracking of lymphocytes in the human body, and neuronal patterning in the developments of nervous system. Misguided cell migration plays a role in a variety of human diseases including metastatic cancer and inflammatory diseases such as asthma and arthritis (Jin et al., 2008; Jin et al., 2009; Charest et al., 2010). Understanding of the fundamental mechanisms underlying cell migration holds the promise of effective therapeutic approaches for treating disease, cellular transplantation, and the preparation of artificial tissues (Ridley et al., 2003). A large family of small proteins, chemokines, serves as the extracellular signals, and a family of G-protein-coupled receptors (GPCRs), chemokine receptors, detects gradients of chemokines and guides cell movement *in vivo*. Currently, 18 chemokine receptors have been identified that mediate responses to more than 50 chemokines (Murphy, 2002). However, relatively little is known about the molecular mechanisms by which these receptors control chemokine-gradient sensing and the directed migration of immune and other cells (Jin et al., 2009).

Cell migration is an integrated process that requires the continuous, coordinated formation and disassembly of cell attachment. The migratory cycle includes extension of an F-actin-mediated protrusion, formation of

stable attachments near the leading edge, translocation of the cell body forward, release of the attachment, and retraction of the cell's posterior (Jeon et al., 2007a).

Over the last 30 years, one such organism, the soil amoeba *Dictyostelium discoideum*, has emerged as a powerful model system for investigating both chemotaxis and phagocytosis (Jin et al., 2009). The first step in chemotaxis is the binding of chemoattractants to the cell surface G-protein coupled receptors (GPCRs). In *Dictyostelium* four cAMP receptors (cAR) have been identified. cAR2-4 have a relative low affinity for cAMP and are important during multicellular stage, whereas cAR1 has a high affinity for cAMP and is essential for signal transduction during early development and chemotaxis (Kortholt A and Haastert, 2008).

Because of their critical role in human oncogenesis Ras proteins have been the subject of intensive research. The *Dictyostelium* Ras GTPase subfamily is comprised of 15 proteins; 11 Ras, 3 Rap, and one Rheb related protein (Kortholt A and Haastert, 2008). Rap1 is the closest homolog of the small GTPase Ras and, like Ras, cycles between an inactive GDP-bound and an active GTP-bound conformation. Rap1 activation or deactivation is regulated by guanine nucleotide exchange factors (GEFs) and GTPase-activating proteins (GAPs), respectively (Fig. 1) (Bos and Zwartkruis, 1999; Bos, 2005).

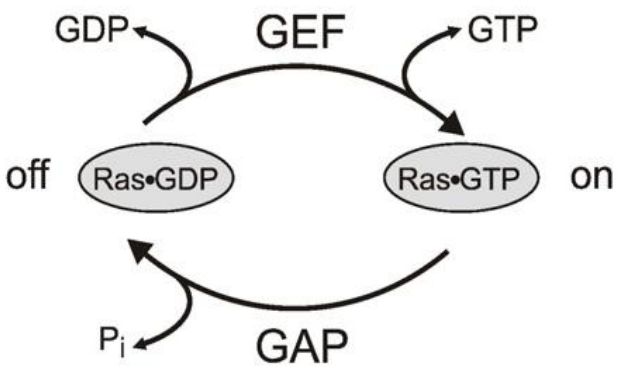

Figure 1. The G-protein cycle.

Small G-proteins switch between an inactive GDP-bound and active GTP-bound state. GEFs (guanine exchange factors) activate GDP-bound Ras by catalysing the exchange of GDP for GTP. Only in the active GTP-bound state, Ras can interact with downstream effectors. GAPs (GTPase activating proteins) catalyse the return to the inactive GDP-state (Kortholt A and Haastert, 2008).

The Rap1 protein has an essential function in integrin-mediated cell adhesion and cadherin-mediated cell-cell adhesion (Kooistra et al., 2007; Scrima et al., 2008; Raaijmakers and Bos, 2009) as well as phagocytosis and cell migration in *Dictyostelium* (Jeon et al., 2007b; Kolsch et al., 2008). Recent reports have demonstrated that Rap1 is rapidly and transiently activated in response to chemoattractant stimulation with activity peaking at ~6 sec after chemoattractant stimulation and the activated Rap1 localizes at the leading edge of chemotaxing cells (Jeon et al., 2007a). The leading-edge activation of Rap1 regulates cell adhesion and helps establish cell polarity by locally modulating MyoII (MyosinII) assembly and disassembly through the Rap1/Phg2 signaling pathway. Spatial and temporal regulation of cell adhesion by Rap1 is required for proper cell migration (Jeon et al., 2007a).

RapGAP1 was recently identified as a specific GAP protein for Rap1 and is involved in the temporal and spatial regulation of Rap1 activity in the anterior of chemotaxing cells to control cell-substratum adhesion and MyoII assembly during chemotaxis (Jeon et al., 2007a). RapGAP3 regulates the levels of Rap1 activation during morphogenesis and, by doing so, mediates the proper sorting of prestalk and prespore cells within the multicellular aggregate by controlling cell-cell adhesion and cell migration (Jeon et al., 2009).

To further examine the regulatory functions of Rap1, I previously undertook a bioinformatics search for potential Rap1 GAPs and identified

10 open reading frames containing a putative RapGAP domain (Jeon et al., 2007a). In this study, I demonstrate that RapGAP9 is involved in morphogenesis, development, and cell adhesion.

II. Materials and Methods

II-1. Materials

I obtained latrunculin B, LY294002 from Sigma-Aldrich, anti-GFP antibodies from Santa Cruz Biotechnology, Inc., 13-mm nitrocellulose filters used for the adhesion assay were obtained from Millipore.

II-2. Cell culture, strains, and plasmid construction

Dictyostelium strains were grown in HL5 axenic media or in association with *Klebsiella aerogenes* at 22℃. The knock-out strains and transformants were maintained in 10 μg/ml blasticidin or 20 μg/ml G418.

The full coding sequence of the *rapGAP9* was generated by PCR and cloned into the *Eco*R I -*Xho* I site of the expression vector pEXP-4(+) containing a GFP fragment (Fig. 2) (Meima et al., 2007).

For expression of truncated RapGAP9 proteins, the various deletion *rapGAP9* sequences were amplified by PCR and cloned into the *Eco*R I - *Xho* I site of an pExp-4(+) vector. I made a *rapGAP9* knockout construct by inserting the blasticidin resistance cassette into the *Bam*H I site created at nucleotide 402 of the *rapGAP9* cDNA, and used it for a gene replacement in the KAx-3 parental strains. Randomly selected clones were screened for a gene disruption by PCR.

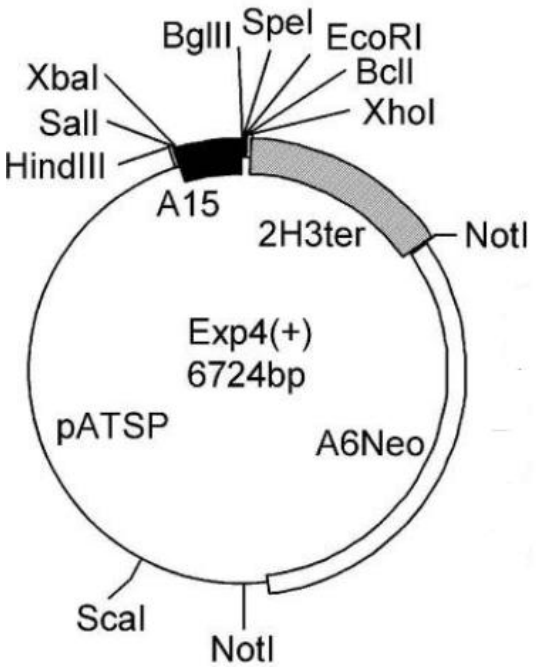

Figure 2. The map of the pExp4(+) plasmid.

The plasmid pEXP4(+) carries the Act6NeoR cassette for G418 selection in *Dictyostelium*, and a cassette for protein expression consisting of the constitutive actin 15 (A15) promoter, the 2H3 terminator, and a small polylinker with 6 restriction sites (Meima et al., 2007).

II-3. Development and chemotaxis analysis.

Exponentially growing cells were harvested and washed twice with 12 mM Na/K phosphate buffer (pH 6.1) and plated on Na/K phosphate agar plates at a density of 3.5 X 10^7 cells /cm^2. The developmental morphology of the cells was examined by photographing the developing cells with a phase-contrast microscope.

The chemotaxis towards cAMP and changes in the subcellular localization of proteins in response to chemoattractant stimulation were examined as described previously (Sasaki et al., 2004; Jeon et al., 2007a). The aggregation-competent cells were prepared by incubating the cells at a density of 5 X 10^6 cells /ml in Na/K phosphate buffer for 10 hr. Cell migration was analyzed using Dunn Chemotaxis Chamber (Hawksley). The images of chemotaxing cells were taken at time-lapse intervals of 6 sec for 30 min using an inverted microscope. The data were analyzed by using NIS-elements software (Nikon).

II-4. Quantitative analysis of GFP fusion proteins

The quantitative analysis of membrane or cortical localization of GFP fusion proteins was performed as described previously (Sasaki et al., 2004; Jeon et al., 2007a; Cha et al., 2010). The aggregation competent cells were allowed to adhere to the plate for 10 min. The cells were uniformly stimulated with cAMP by quickly pipetting 200 μl of 150 μM cAMP into the

plate containing cells. The fluorescence images were taken at time-lapse intervals of 1 sec for 1 min by using an inverted microscope. The frames were captured and analyzed by using NIS-elements software (Nikon) and Image J software (National Institutes of Health).

II-5. Cell attachment assay

Log-phase growing cells on the plates were washed with Na/K phosphate buffer and resuspended at a density of 2 X 10^6 cells /ml. The amount of 4 X 10^5 cells in 200 μl were plated onto 13-mm circular nitrocellulose filters (Millipore). After 30 min, unattached cells were removed by dipping filters into Na/K phosphate buffer. Filters were transferred to microcentrifuge tubes filled with 800 μl Na/K phosphate buffer and vortexed for 1 min with a mixer simultaneously. 150 μl of the detached cells from the filters were plated onto a 30-mm Petri plate with a hole covered by a 0.17-mm glass coverslip, and an additional coverslip was placed on tip. The cells were photographed and counted (detached cell number). To determine the total cell number, 200 μl of the cells was transferred into microcentrifuge tubes filled with 600 μl Na/K buffer and counted. Cell adhesion was presented as a percentage of detached cells compared with total cells. This experiment was repeated three times or more, each time with four filters for each strain.

Ⅱ-6. DAPI staining

Exponentially growing cells were placed on the coverslip and then fixed with 3.7 % formaldehyde for 10 min. The fixed cells were washed with Na/K phosphate buffer, followed by permeabilizing with 0.1 % Triton X-100, drying, and then staining with 0.5 % Hoechst Dye in 1ml of mounting solution Fluoromount-G (SouthernBiotech). Epifluorescence images of random fields of view were captured by using NIS-elements software (Nikon).

Ⅱ-7. RT-PCR

The total RNAs from wild-type cells and *rapGAP9* null cells were extracted by using the SV Total RNA Isolation System (Promega), and the cDNAs were synthesized by reverse transcription with MMLV reverse transcriptase (Promega) using random hexamers and 5 μg of total RNAs. 2 μl of the cDNAs were used in the following PCR with 35 cycles employing gene-specific primers (Table. 1). The universal 18S ribosomal RNA specific primers were used as an internal control (Schroeder et al., 2001; Jeon et al., 2007a).

III. Results

III-1. Identification of the gene encoding RapGAP9

To investigate the pathway leading to Rap1 activation and deactivation, I undertook a bioinformatic search for potential Rap1GAPs and identified nine proteins with a RapGAP domain in the *Dictyostelium* genome sequence database. Figure 3 depicts the domain structure and the derived amino acid sequence of one of these, referred to as RapGAP9 (DDB0233724). *Dictyostelium* RapGAP9 has 366 amino acids (expected molecular mass 41 kDa) and a RapGAP domain at the C-terminal region (Fig. 3A).

To examine the similarity of RapGAP9 with other GAP domain-containing proteins, the amino acid sequence of the GAP domain of RapGAP9 was compared with those of other GAP proteins by multiple alignments. Identical residues were highlighted in dark grey and conserved residues in light grey. Asterisks indicate structurally or catalytically important amino acid residues. The RapGAP9 GAP domain contains the catalytic Asn251 residue (Asn280 in Hs-RapGAP1) required for Rap1 GAP activity, suggesting that RapGAP9 is a *bona fide* RapGAP. The GAP domain of RapGAP9 shares 45.8 % and 41.1 % sequence identities with those of human Rap1GAP and *Dictyostelium* RapGAP3, respectively (Fig. 3B).

The phylogenetic trees with *Dictyostelium* RasGAP/RapGAP containing

proteins and GAP proteins from other organisms show that RapGAP9 is more closely related to the RapGAP family rather than the RasGAP family (Fig. 3C). This suggests that the GAP domain of RapGAP9 might have GAP activity for Rap1 but not other Ras proteins.

A


RapGAP
RapGAP9
171 - 360
366a.a

B

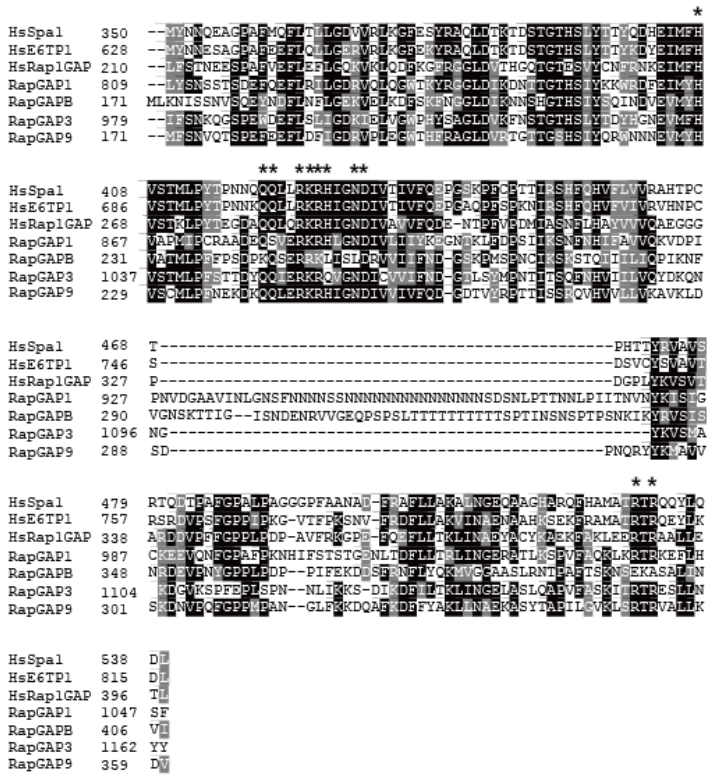
HsSpa1 350
HsE6TP1 628
HsRap1GAP 210
RapGAP1 809
RapGAPB 171
RapGAP3 979
RapGAP9 171
HsSpa1 408
HsE6TP1 686
HsRap1GAP 268
RapGAP1 867
RapGAPB 231
RapGAP3 1037
RapGAP9 229
HsSpa1 468
HsE6TP1 746
HsRap1GAP 327
RapGAP1 927
RapGAPB 290
RapGAP3 1096
RapGAP9 288
HsSpa1 479
HsE6TP1 757
HsRap1GAP 338
RapGAP1 987
RapGAPB 348
RapGAP3 1104
RapGAP9 301
HsSpa1 538
HsE6TP1 815
HsRap1GAP 396
RapGAP1 1047
RapGAPB 406
RapGAP3 1162
RapGAP9 359

C

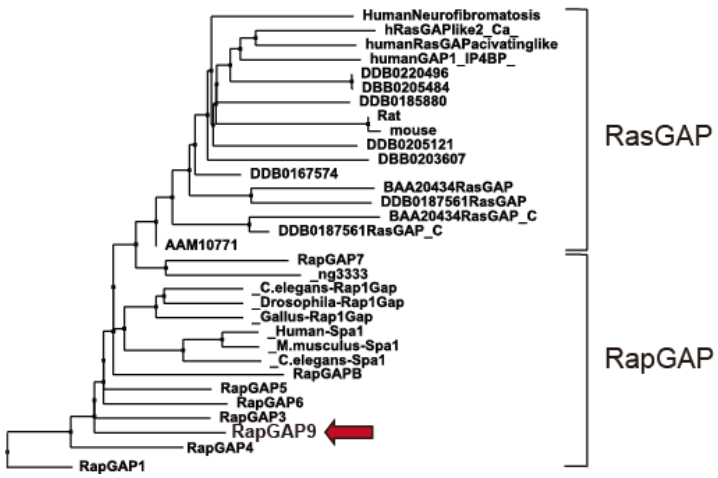
HumanNeurofibromatosis
hRasGAPlike2_Ca_
humanRasGAPactivatinglike
humanGAP1_IP4BP_
DDB0220496
DBB0205484
DDB0185880
Rat
mouse
DDB0205121
DBB0203607
DDB0167574
BAA20434RasGAP
DDB0187561RasGAP
BAA20434RasGAP_C
DDB0187561RasGAP_C
AAM10771
RapGAP7
_ng3333
_C.elegans-Rap1Gap
_Drosophila-Rap1Gap
_Gallus-Rap1Gap
_Human-Spa1
_M.musculus-Spa1
_C.elegans-Spa1
_RapGAPB
RapGAP5
RapGAP6
RapGAP3
RapGAP9
RapGAP4
RapGAP1
RasGAP
RapGAP

Figure 3. Domain structure of RapGAP9 and multiple alignment

(A) Domain structure of the *Dictyostelium* RapGAP9 showing a RapGAP domain in the C-terminus. (B) Multiple alignment of RapGAPs. The amino acid sequence of a GAP domain of RapGAP9 was compared with those of other organisms. HsSpa1, *Homo sapiens* Spa1 (O60618); HsE6TP1, H. Sapiens (Q9UNU4); HsRap1GAP, H. sapiens (P47736); DRapGAP1, *Dictyostelium discoideum* (dictyBaseID: DDB0233726, http://www.dictybase.org/); DRapGAPB, (dictyBaseID: DDB0233728); DRapGAP3, (dictybaseID: DDB0229869); and DRapGAP9, (dictybaseID: DDB0233724). Conserved residues are box shaded, and asterisks indicate the amino acid residues that are structurally or catalytically important. (C) Phylogenetic tree analysis of the GAP domains from *Dictyostelium* and other organisms. A RapGAP domain of *D. discoideum* RapGAP9 displays considerable sequence similarity to human Rap1GAP (45.8 % identity and 64.7 % similarity). Human Neurofibromatosis (P21359); hRasGAPlike2(Ca) (B1AKC7); humanGAP1_IP4BP (Q14644); human RasGAP-activating-like protein 1(O95294); Rat p120GAP, (P50904); Mouse p120GAP (P50904); BAA20434RasGAP (O00899); BAA20434RasGAP_C (O00899); *C. elegans* Rap1GAP (Q86RS9); Human Spa1 (Q96FS4); *Gallus* Rap1GAP (Q5ZMV8); *M. musculus* Spa1 (P46062); *Drosophilia* Rap1GAP (O44090); DRapGAP1 (dictyBaseID: DDB_G0271734); DRapGAPB (dictyBaseID: DDB_G0282247); DRapGAP3 (dictyBaseID: DDB_G0271806); DRapGAP4 (dictyBaseID: DDB_G0291510); DRapGAP5 (dictyBaseID: DDB_G0276549); DRapGAP6

(dictyBaseID: DDB_G0283057); DRapGAP7 (dictyBaseID: DDB_G0284825); DRapGAP8 (dictyBaseID: DDB_G0280527). These sequences are available at www.dictybase.org

III-2. Generation of a *rapGAP9* null cells and the full coding sequence of RapGAP9

To examine the possible roles of RapGAP9 in cell adhesion, cell motility, and morphogenesis *in vivo*, I created *rapGAP9* null strains (*rapGAP9*$^-$ cells) by homologous recombination (Fig. 4A). The *rapGAP9* knockout construct was prepared by inserting the blasticidin resistance cassette into the *rapGAP9* cDNA and used for a gene replacement in KAx-3 parental strains (Fig. 4A). Randomly selected clones were screened for gene disruption by PCR with two sets of primers (Figs. 4A and 4B). In the PCR with tj28/tj29 primers, which are located outside of the BSR cassette in the knock-out construct, and genomic DNAs extracted from wild-type and *rapGAP9* null cells, a band of 1.3 kb was observed in wild-type but not in *rapGAP9* null cells. When another primer tj53, which is located inside of the BSR cassette, instead of tj28 was used in the PCR, only *rapGAP9* null cells showed one clear band of approximately 700 bp, indicating that the *rapGAP9* gene was replaced with the *rapGAP9* knock-out constructs in *rapGAP9* null cells.

To determine whether the *rapGAP9* gene is expressed in rapGAP9 null cells, RT-PCR was performed (Fig. 4C). The cDNAs were synthesized by reverse transcription with total RNAs extracted from wild-type cells and *rapGAP9* null cells and then used in the PCR using *rapGAP9*-specific primer sets. In the PCR with two sets of primers tj28/tj30 and tj28/tj29, there was no band in *rapGAP9* null cells, whereas a band of approximately

400 bp and 1.1 kb, respectively, in wild-type cells. These data confirm that *rapGAP9* is not expressed in *rapGAP9* null cells.

To investigate the roles of RapGAP9 in biological processes, cells overexpressing GFP-RapGAP9 fusion proteins were prepared, and the expression of the protein was confirmed by immunoblotting with anti-GFP antibodies, showing an expected size (68 kDa) of a band (Fig. 4D).

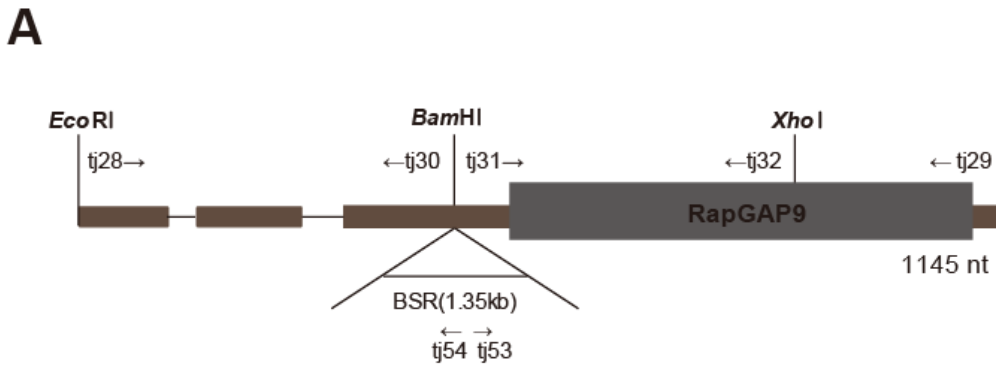
A
EcoRI
BamHI
XhoI
tj28→
←tj30
tj31→
←tj32
←tj29
RapGAP9
1145 nt
BSR(1.35kb)
tj54 tj53

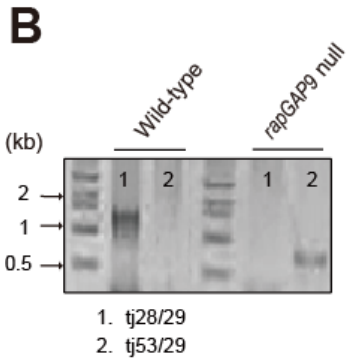
B
Wild-type
rapGAP9 null
(kb)
2
1
0.5
1 2 1 2
1. tj28/29
2. tj53/29

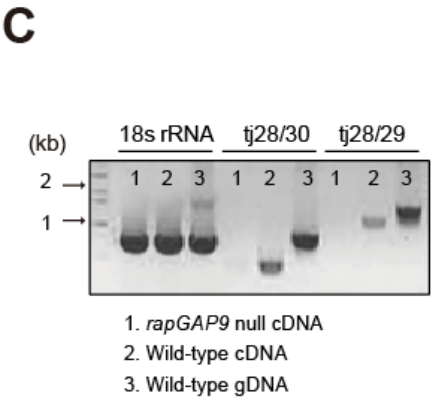
C
(kb)
18s rRNA
tj28/30
tj28/29
2
1
1 2 3 1 2 3 1 2 3
1. rapGAP9 null cDNA
2. Wild-type cDNA
3. Wild-type gDNA

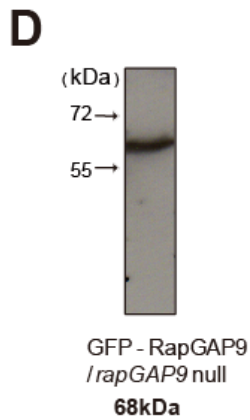
D
(kDa)
72
55
GFP - RapGAP9
/ rapGAP9 null
68kDa

Figure 4. *rapGAP9* knock-out constructs and confirmation of the deletion of the gene.

(A) *rapGAP9* knock-out constructs. The locations of the primers used in the PCRs for screening *rapGAP9* null cells and the position of the inserted BSR cassette are illustrated. (B) Confirmation of gene replacement in *rapGAP9* null cells. Genomic DNAs from wild-type cells and *rapGAP9* null cells were extracted and used in PCR using two sets of primers. (C) Examination of the expression of *rapGAP9* in *rapGAP9* null cells by RT-PCR. Total RNAs extracted from wild-type cells and *rapGAP9* null cells were used in RT-PCR. The universal 18S ribosomal RNA specific primers were used as an internal control (Schroeder et al., 2001; Jeon et al., 2007a). The genomic DNAs extracted from wild-type cells were used for clarifying the amplification from the cDNAs in PCR. (D) Western blot analysis of GFP-RapGAP9. *rapGAP9* null cells expressing GFP-RapGAP9 were subjected to immunoblotting with an anti-GFP antibody.

Table 1. PCR primer sequences used for knockout screening

Primer	Sequence	Location
	5'→3'-directed PCR primers	
tj28	ATGATTGCGCCAGCTGTAGG	1-20
tj31	GATCCAAGAATATCA	403-417
tj53	TTTTAAAAAAAATAGATCTCCTAGG	BSR
	3'→5'-directed PCR primers	
tj29	TGATTATTTAACAAAAGCTTC	1084-1101
tj32	TGCGGGCATTGGTGGACC	925-942
tj54	GAATTAGTAGAAGTAGCGACAGAGAAGA	BSR

III-3. RapGAP9 is involved in the regulation of cytoskeleton and cytokinesis

To address the function of RapGAP9 in cells, I examined the morphology of *rapGAP9* null cells and RapGAP9-overexpressing cells. Compared to wild-type cells, some of *rapGAP9* null cells were more flat and spread out, and highly multinucleated. Examination of the number of nucleus with Hoechst dye showed *rapGAP9* null cells have a cytokinesis defect. Majority of wild-type cells contained one nucleus, whereas most of *rapGAP9* null cells had two nuclei and some of the cells over eight nuclei (Figs. 5B and 5C). The introduction of RapGAP9 into *rapGAP9* null cells rescued the cytokinesis defect of the null cells and the *rapGAP9* null cells expressing RapGAP9 showed normal number of nucleus. These results suggest that RapGAP9 plays an important role in cytokinesis.

Cells expressing constitutively active Rap1 display flat, spread morphology, and strong attachment to the substratum (Jeon et al., 2007b). *rapGAP9* null cells exhibited similar morphological phenotypes to the cells expressing constitutively active Rap1. Compared to wild-type cells, *rapGAP9* null cells were more flat and spread out, displayed more filopodia, and showed strong attachment to the substratum. Measuring the cell size using NIS-element software with a four point elliptical function showed that the mean cell size of the *rapGAP9* null cells was approximately 5-fold larger than wild-type cells (Fig. 6B). The morphological phenotype of *rapGAP9* null cells was complemented by expressing of RapGAP9,

suggesting a function of RapGAP9's on the cell shape formation.

To examine the possible roles of RapGAP9 in cell adhesion, I measured the fraction of cells that detach from a membrane during agitation. *rapGAP9* null cells showed strong attachment compared to wild-type cells and this was partially complemented in GFP-RapGAP9 overexpressing cells (Fig. 6C). I then investigated the effect of RapGAP9 on chemoattractant-mediated reorganization of the cytoskeleton (Fig. 6D). Wild-type cells exhibited a transient and rapid F-actin polymerization with a peak at 5 seconds in response to chemoattractant stimulation. The loss of RapGAP9 resulted in 1.5-fold increase in the basal level of F-actin. However, the kinetics of the response was similar to those of wild-type cells with the level of F-actin proportionally higher in *rapGAP9* null cells. These data suggest that RapGAP9 is involved in reorganizing the cytoskeleton and cell-substratum attachment.

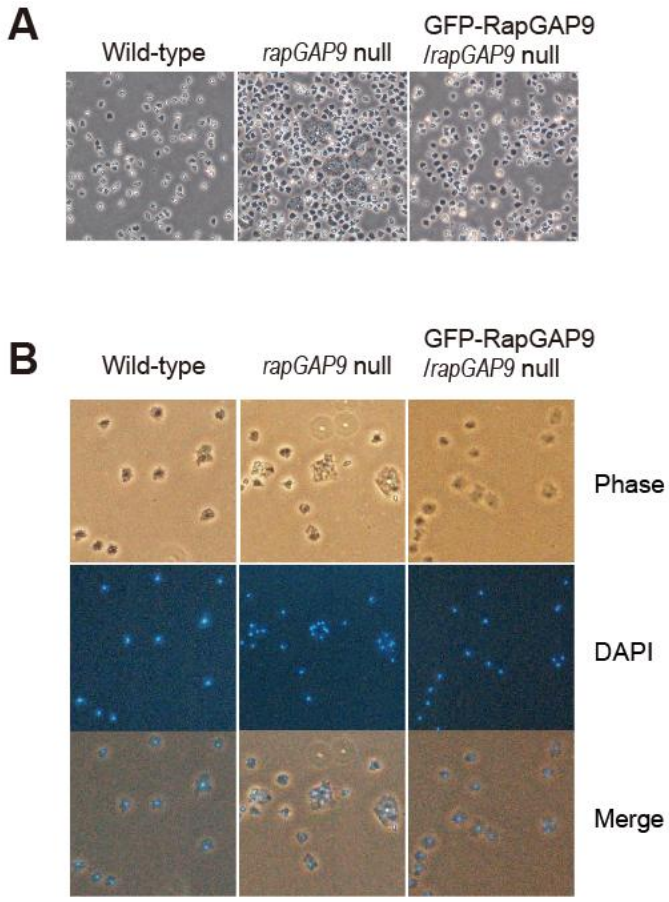
A
Wild-type
rapGAP9 null
GFP-RapGAP9
/rapGAP9 null
B
Wild-type
rapGAP9 null
GFP-RapGAP9
/rapGAP9 null
Phase
DAPI
Merge
C
*
Nuclei number
0
1
2
3
4
Wild-type
rapGAP9 null
GFP-RapGAP9
/rapGAP9 null
Fraction of
total measurements
0
10
20
30
40
50
60
0
1
2
4
8
16
Nuclei / Cell
Wild-type
rapGAP9 null
GFP-RapGAP9
/rapGAP9 null

Figure 5. The cytokinesis defect of *rapGAP9* null cells

(A) Morphology of the cells. Exponentially growing wild-type, *rapGAP9* null cells, and *rapGAP9* null cells expressing GFP-RapGAP9 were photographed. (B) Representative DAPI images of the cells. Corresponding phase-contrast and merged images are shown on the top and bottom panels, respectively. (C) Quantitative analysis of the number of nucleus in the cells. Mean values of the number of nuclei were graphed on the upper part and the frequency distribution was compared on the lower part. Error bars represent SD. Statistically different from control at $^{*}p<0.05$ by the student's t-test.

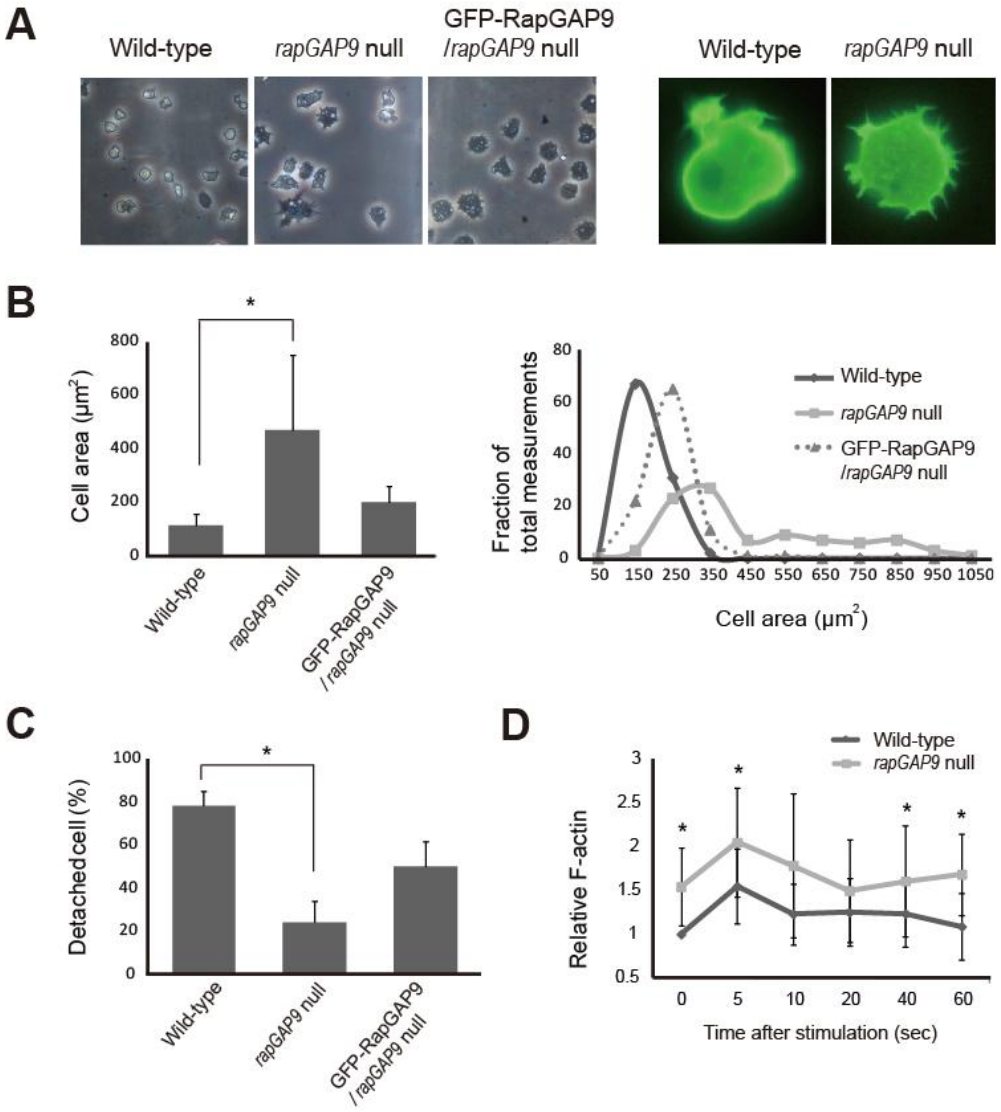
A
Wild-type
rapGAP9 null
GFP-RapGAP9
/rapGAP9 null
Wild-type
rapGAP9 null
B
Cell area (μm²)
800
600
400
200
0
*
Wild-type
rapGAP9 null
GFP-RapGAP9
/rapGAP9 null
Fraction of
total measurements
80
60
40
20
0
Wild-type
rapGAP9 null
GFP-RapGAP9
/rapGAP9 null
50 150 250 350 450 550 650 750 850 950 1050
Cell area (μm²)
C
Detached cell (%)
100
80
60
40
20
0
*
Wild-type
rapGAP9 null
GFP-RapGAP9
/rapGAP9 null
D
Relative F-actin
3
2.5
2
1.5
1
0.5
*
*
*
*
Wild-type
rapGAP9 null
0 5 10 20 40 60
Time after stimulation (sec)

Figure 6. Cell spreading, cell adhesion, and F-actin assembly of *rapGAP9* null cells

(A) Spreading morphology of vegetative cells. Wild-type and *rapGAP9* null cells expressing GFP-ABP were imaged (on the right) to observe the filopodia in the cells. (B) Analysis of the cell area (left) and frequency distribution of the cell area (right). (C) Cell-substratum adhesion. Adhesion was measured by the ratio of detached cells to the total number of cells. Experiments were performed at least three times. (D) Kinetics of F-actin polymerization in response to chemoattractant stimulation. Error bars represent SD. Statistically different from control at $^{*}p<0.05$ by the student's t-test.

Ⅲ-4. RapGAP9 is required for proper cell migration and development

The previous sequence analysis showed the homology of RapGAP9 with RapGAP1 and RapGAP3, which are required for proper cell migration through the regulation of Rap1 activity in *Dictyostelium* (Jeon et al., 2007a; Jeon et al., 2009). In addition, the phenotypes of *rapGAP9* null cells are very similar to those of cells expressing constitutively active Rap1. These data raised a possibility of involvement of RapGAP9 in cell migration and developmental process in *Dictyostelium*. Therefore, I examined the ability of *rapGAP9* null cells to polarize and chemotax up a cAMP chemoattractant gradient using Image J software and NIS-element software. In response to uniform stimulation with chemoattractants, wild-type cells became highly elongated, polarized, and moved fast (average speed of approximately 15 μm/min). In contrast, *rapGAP9* null cell were polarized, but the moving speed was slightly lower than that of wild-type cells (Fig. 7). In addition, the directionality, which is a measure of how straight the cells move, of *rapGAP9* null cells was lower than wild-type cells (Fig. 7). These data suggest that RapGAP9 is required for proper cell migration and possibly involved in directional sensing during chemotaxis.

During development in *Dictyostelium*, cells release cAMP, causing surrounding cells to migrate and initiate the formation of a multicellular fruiting body (Chisholm RL, 2004). To examine the possible roles of RapGAP9 in development, I performed a development assay. *rapGAP9* null

cells aggregated normally to form a mound at ~8 hr, with a timing and morphology similar to wild-type cells (Fig. 8A). However, the formation of the fruiting body was slightly delayed in *rapGAP9* null cells, and *rapGAP9* null cells had spores 40% smaller compared to wild type (Fig. 8B). Expression of GFP-RapGAP9 in *rapGAP9* null cells complemented the developmental phenotypes of *rapGAP9* null cells, with developmental timing and morphologies similar to the parental wild-type strain. These results indicate RapGAP9 is required for proper development. The growth of the *rapGAP9* null strain was indistinguishable from wild-type cells in suspension (Fig. 8C).

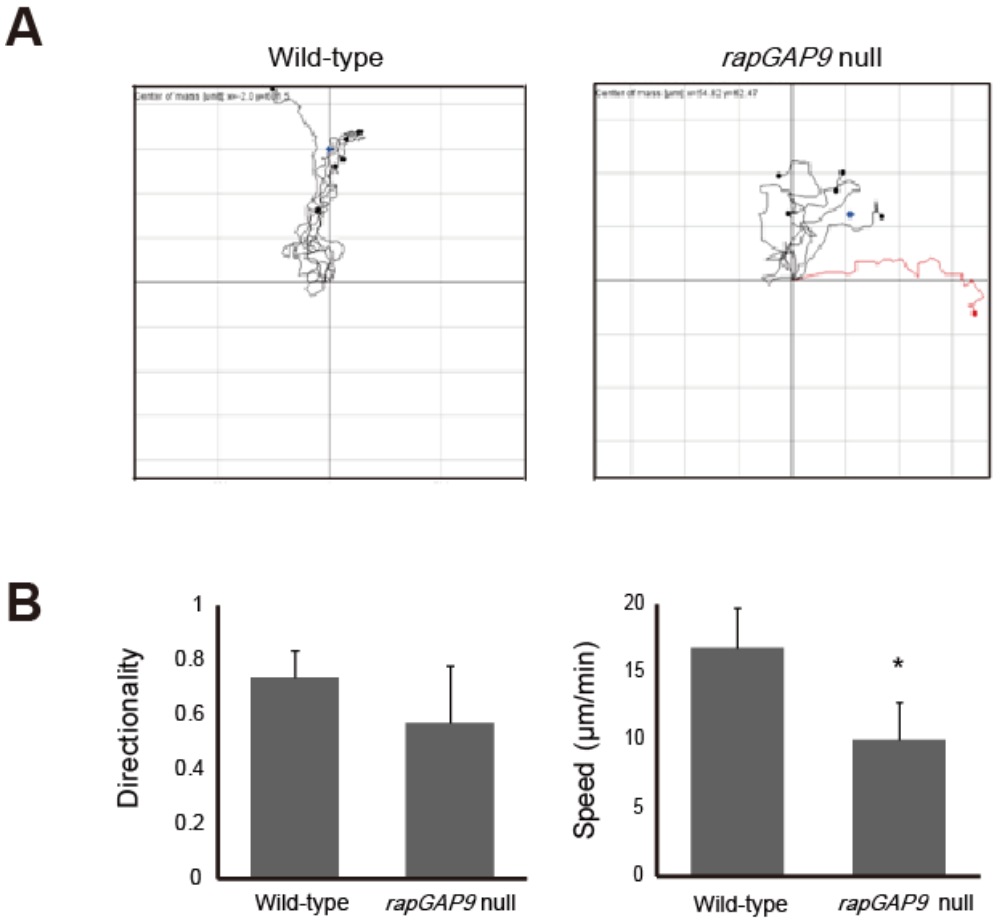
A
Wild-type
rapGAP9 null
B
Directionality
1
0.8
0.6
0.4
0.2
0
Wild-type
rapGAP9 null
Speed (µm/min)
20
15
10
5
0
*
Wild-type
rapGAP9 null

Figure 7. Chemotaxis of *rapGAP9* null cells.

Aggregation-competent cells from wild-type or *rapGAP9* null cells were placed in a Dunn chemotaxis chamber, and the movements of the cells up a chemoattractant (cAMP) gradient were recorded by time lapse photography for 30 min at 6 sec intervals. (A) Trajectories of cells migrating toward cAMP in Dunn chemotaxis chamber. Trajectories were tracked with ImageJ software. Each line represents the track of a single cell chemotaxing toward cAMP (150 μM). (B) Analysis of chemotaxing cells. The recorded images were analyzed by NIS-element software. Directionality is a measure of how straight the cells move. Cells moving in a straight line have a directionality of 1.0. It is calculated as the distance moved over the linear distance between the start and the finish. Wild-type cells show a significantly higher directional movement towards an apical region of the organism than *rapGAP9* null cells. Speed indicates the speed of the cell's movement along the total path. Error bars represent SD. Statistically different from control at $^{*}p<0.05$ by the student's t-test.

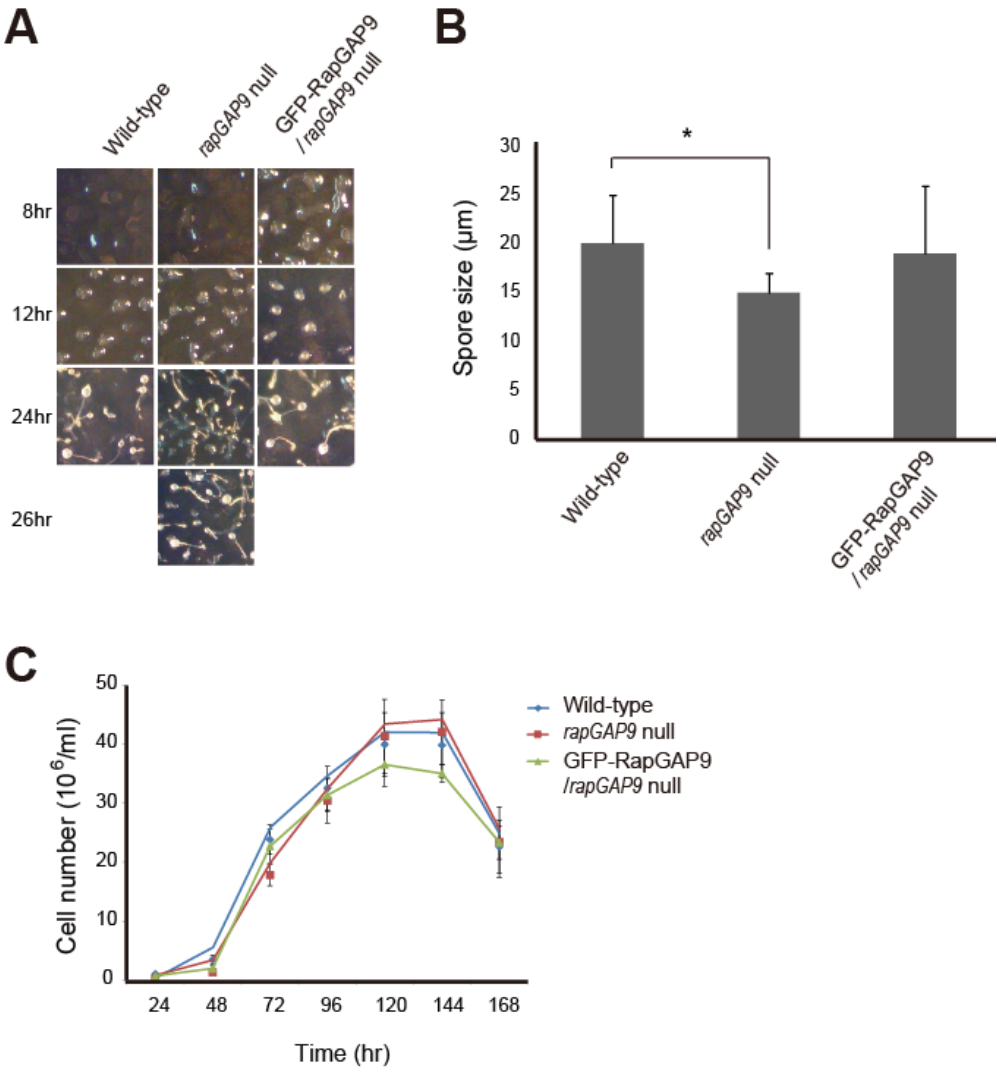
A
Wild-type
rapGAP9 null
GFP-RapGAP9 / rapGAP9 null
8hr
12hr
24hr
26hr
B
Spore size (μm)
30
25
20
15
10
5
0
*
Wild-type
rapGAP9 null
GFP-RapGAP9 / rapGAP9 null
C
Cell number (10^6/ml)
50
40
30
20
10
0
24
48
72
96
120
144
168
Time (hr)
Wild-type
rapGAP9 null
GFP-RapGAP9 /rapGAP9 null

Figure 8. Development of *rapGAP9* null cells and the cells overexpressing RapGAP9

(A) Developmental morphology of *rapGAP9* null cells and cells expressing GFP-RapGAP9. Vegetative cells were washed and plated on non-nutrient agar plates. Photographs were taken at the times indicated after plating. Developmental images of the cells at 8 hr (wild-type early mound stage), 12 hr (wild-type tip forming stage), 24 hr (wild-type fruiting body stage) are shown. Development of *rapGAP9* null cells was delayed. (B) Analysis of the size of the fruiting bodies at 24 hr. *rapGAP9* null cells has smaller spores compared to wild type cells. (C) Growth rates of the cells in suspension culture. KAx-3, *rapGAP9* null, and GFP-RapGAP9/*rapGAP9* null strains were transferred from the growing plates into axenic shaking culture medium and then counted at intervals thereafter. The plotted values are the means of duplicate cell counts. Experiments were performed at least three times. Error bars represent SD. Statistically different from control at $^{*}p<0.05$ by the student's t-test.

III-5. Subcellular localization of GFP-RapGAP9

To examine the dynamic localization of RapGAP9, I expressed GFP-fusion RapGAP9 and truncated proteins in wild-type or *rapGAP9* null cells (Fig. 9A). GFP-RapGAP9 was found at the cell cortex in resting cells, and truncated RapGAP9 proteins (lacking either the GAP domain or the N-terminus) were observed at the cytosol (Fig. 9B), suggesting that the GAP domain and the N-terminus are required for the cell cortex localization of RapGAP9. Upon uniform chemoattractant stimulation, GFP-RapGAP9 in the cytosol transiently translocated to the cortex with a peak at ~7 sec, similar to the kinetics for RapGAP1 (Fig. 9C) (Jeon et al., 2007a). In migrating cells, RapGAP9 localized preferentially at the leading edge (Fig. 9E). I then compared the translocation kinetics of GFP-RapGAP9 to the cell cortex with those of GFP-ArpD. The kinetics of GFP-RapGAP9 translocation were several seconds slower than those of GFP-ArpD (Fig. 9C), suggesting that RapGAP9 localization might correlate with the termination of F-actin polymerization.

To investigate the mechanism for the cell cortex localization of RapGAP9, the localization of RapGAP9 in the presence of latrunculin B (an inhibitor of actin polymerization) and a PI3K inhibitor (LY294002) was examined. When the cells were treated with latrunculin B, cells became round and appeared to lose pseudopodia in the plasma membrane, and ArpD-GFP (used as a control protein to binds to F-actin) was dissociated from the membrane. However, RapGAP9 was still uniformly associated with the plasma

membrane in the presence of latrunculin B, suggesting a presence of F-actin independent mechanism for RapGAP9 localization at the cell cortex. Next, I determined whether the cell cortex localization of RapGAP9 is dependent on PI3K signaling by using a PI3K inhibitor LY294002. LY294002 treatment resulted in dissociation of phdA-GFP (a PIP3-binding protein used as a control), but RapGAP9 was observed at the cell cortex (Fig. 9D). When cells were simultaneously treated with latrunculin B and LY294002, RapGAP9 disappeared from the plasma membrane (Fig. 9D). These results suggest the cell cortex localization of RapGAP9 uses two mechanisms, one F-actin dependent and the other PI3K-signaling dependent.

To determine whether GFP-RapGAP9 binds to lipids, I performed lipid-binding assays *in vitro*. In the lipid-binding assay, supernatants containing the fusion proteins were incubated with nitrocellulose membranes spotted with 15 unique phospholipids (Fig. 9F). Interactions between the fusion protein and lipid were detected using anti-GFP antibodies. GFP-RapGAP9 showed interaction with several lipids, PI(3)P, PI(4)P, PI(5)P, PI(3,4)P_2, PI(3,5)P_2, PI(4,5)P_2, PI(3,4,5)P_3, and PA. An analysis of these results is currently in progress.

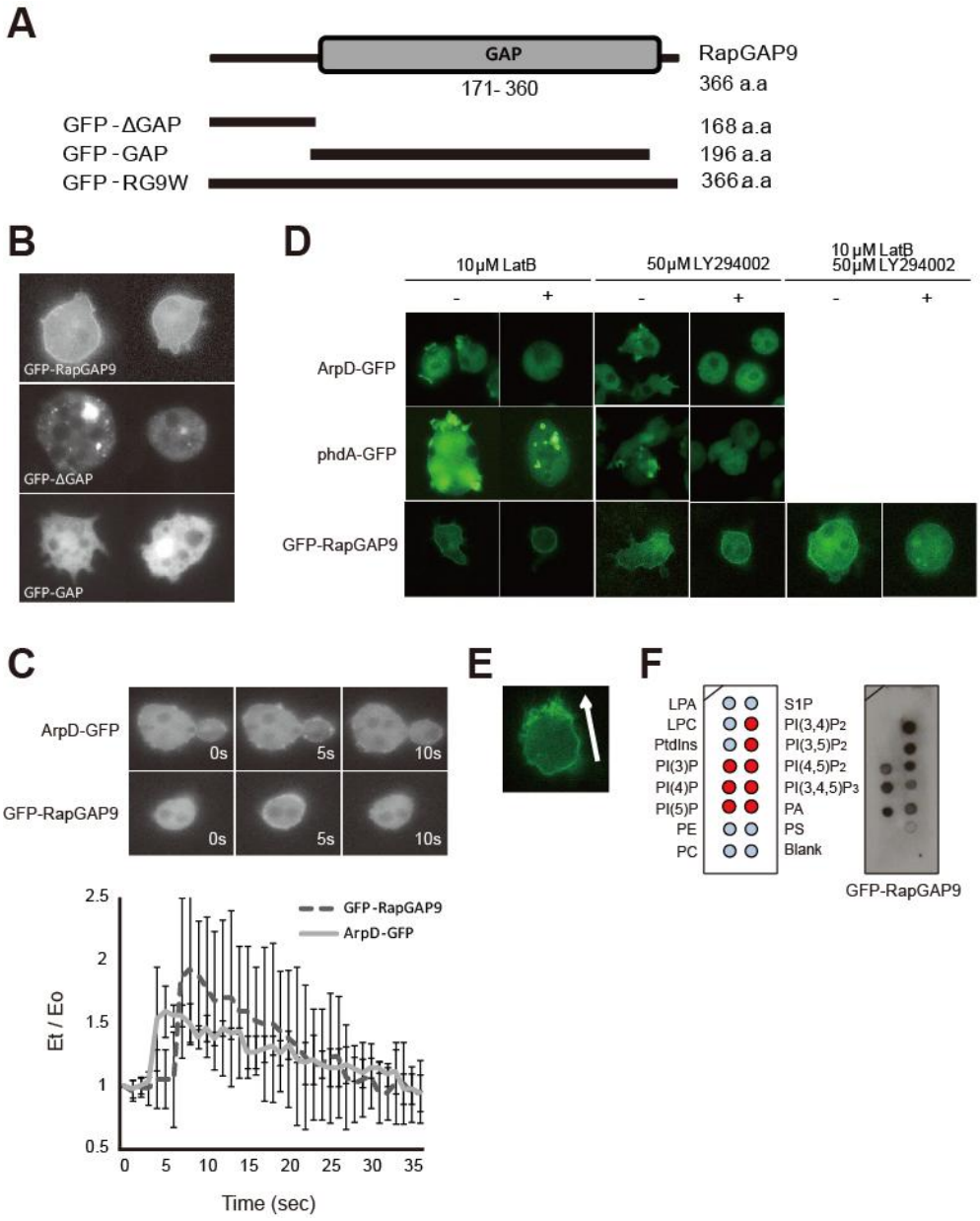
A
GAP
171- 360
RapGAP9
366 a.a
GFP - ΔGAP
168 a.a
GFP - GAP
196 a.a
GFP - RG9W
366 a.a
B
GFP-RapGAP9
GFP-ΔGAP
GFP-GAP
D
10μM LatB
50μM LY294002
10 μM LatB
50μM LY294002
- + - + - +
ArpD-GFP
phdA-GFP
GFP-RapGAP9
C
ArpD-GFP
GFP-RapGAP9
0s
5s
10s
GFP-RapGAP9
ArpD-GFP
Et / Eo
Time (sec)
E
F
LPA
LPC
PtdIns
PI(3)P
PI(4)P
PI(5)P
PE
PC
S1P
PI(3,4)P2
PI(3,5)P2
PI(4,5)P2
PI(3,4,5)P3
PA
PS
Blank
GFP-RapGAP9

Figure 9. Localization of RapGAP9.

(A) Diagram of the truncated GFP-fusion RapGAP9 proteins. (B) Localization of GFP-RapGAP9, GFP-GAP, GFP-ΔGAP in *rapGAP9* null cell. (C) Translocation of GFP-RapGAP9 in wild-type cells to the cell cortex in response to uniform chemoattractant stimulation (up panel). Translocation kinetics was analyzed from time-lapse recordings (down panel). The frames were captured using NIS-elements software (Nikon) and analyzed using ImageJ software (National Institutes of Health). The intensity of cortical GFP was measured and the level of cortical GFP was calculated by dividing the intensity before stimulation (Eo) by the intensity at each time point (Et). (D) Localization of ArpD-GFP, phdA-GFP, and GFP-RapGAP9 were analyzed by fluorescence microscopy in presence or absence of 10 μM latrunculinB (LatB) and 50 μM LY294002 (LY). (E) Localization of GFP-RapGAP9 during random movement. The arrow indicates the direction of movement. (F) Dot blot assays for phosphoinositide binding. Supernatants were incubated with dot blots containing a variety of lipids, as indicated in the key to the left. Bound proteins were detected with anti-GFP antibody. LPA; Lysophosphatidic acid, LPC; Lysophosphocholine, PtdIns; Phosphatidylinositol, PI(3)P; Phosphatidylinositol (3) phosphate, PI(4)P; Phosphatidylinositol (4) phosphate, PI(5)P; Phosphatidylinositol (5) phosphate, PE; Phosphatidylethanolamine, PC; Phosphatidylcholine, S1P; Sphingosine 1-Phosphate, PI(3,4)P_2; Phosphatidylinositol (3,4) bisphosphate, PI(3,5)P_2; Phosphatidylinositol (3,5) bisphosphate, PI(4,5)P_2;

Phosphatidylinositol (4,5) bisphosphate, PI(3,4,5)P3; Phosphatidylinositol (3,4,5) trisphosphate, PA; Phosphatidic acid, PS ;Phosphatidylserine.

IV. Discussion

The small GTPase Rap1 is involved in the control of diverse cellular processes including integrin-mediated cell adhesion, cadherin-based cell-cell adhesions, cell polarity formation, and cell migration. The putative Rap1 GAP domain of RapGAP9 showed high sequence homology with those of other GAP-domain containing proteins in other organism. Loss of RapGAP9 resulted in an altered morphology of fruiting body. *rapGAP9* null cells were multinucleated and have a cytokinesis defect. Also, RapGAP9 is involved in reorganizing the cell cytoskeleton and cell-substratum attachment. RapGAP9 full length was required for localized cell cortex and binds plasma membrane *via* F-actin and PI3K pathway.

RapGAP9 regulates cell attachment and cell spreading

I examined the function of a member of *Dictyostelium* GAP proteins for Rap1, referred to RapGAP9, in regulation of Rap1 and cell migration. Rap1 is involved in integrin-mediated cell adhesion and modulates integrin avidity and affinity (Webb et al., 2002). In *Dictyostelium*, Rap1 is a key molecule controlling cell adhesion and localizes to intracellular membranes and to the plasma membrane as well (Jeon et al., 2007b). *rapGAP9* null cells are flatten and exhibit strong adhesion to the substratum as observed in cells expressing constitutively active Rap1G12V (Figs. 6A-C) (Jeon et al., 2007b). These phenotypes in *rapGAP9* null cells were complemented by

expressing RapGAP9. These phenotypes are also observed in cells with high level of Rap1 activity. Cells overexpressing GbpD, which is a Rap1-specific GEF protein, are spread and exhibit strongly increased cell-substrate attachment (Kortholt A and Haastert, 2008), supporting that *rapGAP9* null cells might have a high level of Rap1 activity resulting in spreading morphological phenotypes.

RapGAP9 is involved in filopodia formation and cytokinesis

Wild-type cells exhibit a biphasic F-actin polymerization profile with a sharp peak at 5 sec and a second lower, broader peak linked to pseudopod extension at ~45-60 sec (Hall et al., 1989). *rapGAP9* null cells have a slightly elevated basal level of F-actin and a proportionally elevated second peak (Fig. 6D). These data are consistent with the phenotypes of *rapGAP1* null cells or Rap1CA cells (Jeon et al., 2007a; Jeon et al., 2007b).

Cytokinesis in eukaryotic organisms is under the intricate control of small GTP-binding proteins of the Ras and Rho families (Glotzer, 1997; Field et al., 1999; Prokopenko et al., 2000), the underlying molecular mechanisms remained largely elusive. The role of Ras protein in cytokinesis has been demonstrated so far only in *Dictyostelium* (Tuxworth et al., 1997). The involvement of Ras in cytokinesis may be restricted to one or a few phylogenetic groups, since extensive studies of Ras proteins in higher eukaryotes have not provided evidence for their role in cytokinesis (Prokopenko et al., 2000). The phenotype of the *rapGAP9* null cells

suggests that RapGAP9 may be involved in mediating cytokinesis (Fig. 5B). Future studies are needed to determine the precise role of specific GTPase and/or other signaling molecules that are required for the recruitment to the cleavage furrow.

RapGAP9 is essential for normal development

Present studies demonstrate that RapGAP9 plays a crucial role in the formation of the fruiting bodies. RapGAPB and RapGAP3 have been identified to control cell morphology during multicellular development (Jeon et al., 2009; Parkinson K, 2009). RapGAP1 plays an important role in chemotaxis at the leading edge of moving cells but appears to play no role in development. RapGAP9 is likely to be involved in the late stage of development (Fruiting body formation stage) (Figs. 8A and 8B). These data suggest that *Dictyostelium* has evolved a complex regulatory mechanism to control the activity of Rap1 at different stages of development through the differential function of a series of RapGAPs.

Localization of RapGAP9 at the cell cortex

Polymerization of the actin cytoskeletal network drives the initial extension of the plasma membrane at the cell front during cell migration. Proteins that regulate actin dynamics and organization, such as vasodilator-stimulated phosphoprotein (VASP), Wiskott-Aldrich syndrome protein (WASP), profiling and the Arp2/3 complex, localize to the periphery

of protruding lamellipodia (Webb et al., 2002). Actin polymerization in lamellipodia is mediated by the Arp2/3 complex, which is activated by WASP/WAVE family members and inhibited by association with coronin.

In this study, GFP-RapGAP9 was observed at the cortex. Upon uniform chemoattractant stimulation, RapGAP9 transiently and rapidly translocated to the cortex. In migrating cells, RapGAP9 preferentially localizes to the leading edge. I found that both the N-terminus and GAP domain of RapGAP9 are required for localized cell cortex, and that the translocation of RapGAP9 to the cell cortex in response to chemoattractant stimulation is mediated by possibly two mechanisms, one F-actin dependent and the another PI3K-pathway dependent.

Conclusion

Cell movement is a coordinated process of F-actin-mediated protrusions at the leading edge and myosin-mediated contraction of the rear of a cell. Rap1 is emerging as a major regulator of cytoskeleton reorganization and cell adhesion in *Dictyostelium*. Rap1 plays important roles in the dynamic control of cell adhesion by regulating the cytoskeleton during cell migration. Identification and characterization of RapGAP9 in this study will provide further insight into the molecular mechanisms through which Rap1 controls cell adhesion during chemotaxis.

V. References

Bos, J. L. (2005). Linking Rap to cell adhesion. *Curr Opin Cell Biol* 17(2): 123-128.

Bos, J. L. and F. J. Zwartkruis (1999). Signal transduction. Rhapsody in G proteins. *Nature* 400(6747): 820-821.

Cha, I., S. H. Lee and T. J. Jeon (2010). Chemoattractant-mediated Rap1 activation requires GPCR/G proteins. *Mol Cells* 30(6): 563-567.

Charest, P. G., Z. Shen, A. Lakoduk, A. T. Sasaki, S. P. Briggs and R. A. Firtel (2010). A Ras signaling complex controls the RasC-TORC2 pathway and directed cell migration. *Dev Cell* 18(5): 737-749.

Chisholm RL, F. R. (2004). Insights into morphogenesis from a simple developmental system. *Nature reviews. Molecular cell biology* 531-41(5(7)).

Field, C., R. Li and K. Oegema (1999). Cytokinesis in eukaryotes: a mechanistic comparison. *Curr Opin Cell Biol* 11(1): 68-80.

Glotzer, M. (1997). The mechanism and control of cytokinesis. *Curr Opin Cell Biol* 9(6): 815-823.

Hall, A. L., V. Warren and J. Condeelis (1989). Transduction of the chemotactic signal to the actin cytoskeleton of *Dictyostelium discoideum*. *Dev Biol* 136(2): 517-525.

Jeon, T. J., D. J. Lee, S. Lee, G. Weeks and R. A. Firtel (2007a). Regulation of Rap1 activity by RapGAP1 controls cell adhesion at the front of chemotaxing cells. *J Cell Biol* 179(5): 833-843.

Jeon, T. J., D. J. Lee, S. Merlot, G. Weeks and R. A. Firtel (2007b). Rap1 controls cell adhesion and cell motility through the regulation of myosin II. *J Cell Biol* 176(7): 1021-1033.

Jeon, T. J., S. Lee, G. Weeks and R. A. Firtel (2009). Regulation of *Dictyostelium* morphogenesis by RapGAP3. *Dev Biol* 328(2): 210-220.

Jin, T., X. Xu, J. Fang, N. Isik and B. J. Yan J, Hereld D. (2009). How human leukocytes track down and destroy pathogens: lessons learned from the model organism *Dictyostelium discoideum*. *Immunol Res.* 118-27(43(1-3)).

Jin, T., X. Xu and D. Hereld (2008). Chemotaxis, chemokine receptors and human disease. *Cytokine* 44(1): 1-8.

Kolsch, V., P. G. Charest and R. A. Firtel (2008). The regulation of cell motility and chemotaxis by phospholipid signaling. *J Cell Sci* 121(Pt 5): 551-559.

Kooistra, M. R., N. Dube and J. L. Bos (2007). Rap1: a key regulator in cell-cell

junction formation. *J Cell Sci* 120(Pt 1): 17-22.

Kortholt A and V. Haastert (2008). Highlighting the role of Ras and Rap during *Dictyostelium* chemotaxis. *Cellular signaling*.

Meima, M. E., K. E. Weening and P. Schaap (2007). Vectors for expression of proteins with single or combinatorial fluorescent protein and tandem affinity purification tags in *Dictyostelium*. *Protein Expr Purif* 53(2): 283-288.

Murphy, P. M. (2002). International Union of Pharmacology. XXX. Update on chemokine receptor nomenclature. *Pharmacol Rev* 54(2): 227-229.

Parkinson K, B. P., Traynor D, Aldren NL, Kay RR, Weeks G, Thompson CR. (2009). Regulation of Rap1 activity is required for differential adhesion, cell-type patterning and morphogenesis in Dictyostelium. *Journal of Cell science* 335-44(122 (pt 3)).

Prokopenko, S. N., R. Saint and H. J. Bellen (2000). Untying the Gordian knot of cytokinesis. Role of small G proteins and their regulators. *J Cell Biol* 148(5): 843-848.

Raaijmakers, J. H. and J. L. Bos (2009). Specificity in Ras and Rap signaling. *J Biol Chem* 284(17): 10995-10999.

Ridley, A. J., M. A. Schwartz, K. Burridge, R. A. Firtel, M. H. Ginsberg, G. Borisy, J. T. Parsons and A. R. Horwitz (2003). Cell migration: integrating signals from front to back. *Science* 302(5651): 1704-1709.

Sasaki, A. T., C. Chun, K. Takeda and R. A. and Firtel (2004). Localized Ras signaling at the leading edge regulates PI3K, cell polarity, and directional cell movement. *The Journal of Cell Biology* 505-518.

Schroeder, S., S. H. Kim, W. T. Cheung, K. Sterflinger and C. Breuil (2001). Phylogenetic relationship of Ophiostoma piliferum to other sapstain fungi based on the nuclear rRNA gene. *FEMS Microbiol Lett* 195(2): 163-167.

Scrima, A., C. Thomas, D. Deaconescu and A. Wittinghofer (2008). The Rap-RapGAP complex: GTP hydrolysis without catalytic glutamine and arginine residues. *EMBO J* 27(7): 1145-1153.

Tuxworth, R. I., J. L. Cheetham, L. M. Machesky, G. B. Spiegelmann, G. Weeks and a. R. H. Insall (1997). Dictyostelium RasG is required for normal motility and cytokinesis, but not growth. *The Journal of Cell Biology* 138: 605-614.

Vl. Acknowledgements

학위 논문심사를 다 마치고 벌써 졸업을 앞두고 있습니다. 많이 힘들었고 실험결과가 뜻대로 안 나올 때는 속상했지만 열심히 하고 나니 저 자신이 많이 성장한 게 느껴집니다. 석사과정을 마치기까지 주변의 도움이 없었다면 많이 힘들었을 것입니다. 우선 걱정 없이 석사까지 할 수 있게 뒷바라지 해주신 부모님 감사합니다. 발표 준비 할 때마다 항상 옆에서 배려해준 내 동생들 혜원이, 정석이 고맙다. 2년 동안 부족한 저를 믿고 이끌어주신 전택중 교수님께 감사 드리며, 논문 심사 해주신 김영곤 교수님, 이준식 교수님 감사 드립니다. 많은 지도와 가르침 주신 박현용 교수님, 최영복 교수님, 조광원 교수님 감사 드립니다.

대학원 다니는 동안 친구라는 것만으로도 나에게 많은 위로가 되고 힘이 된 내 친구들 설, 유나, 현승 이제 자주 만나서 놀자 내 마음 알지? 우리 현승이 나 영어 쓸 때 도움 많이 줘서 고마워. 혜지랑 수현이도 얼른 보고 싶다. 언제 봐도 어제 본 것 같은 재완이 종민이도 힘들 때마다 든든하게 옆에 있어줘서 고맙다. 우리 선미, 누리, 세현이 다들 바빠서 날짜 맞추기 힘들지만 내 활력소들! 우리 스트레스 또 한방에 풀게 만나요~ 누리도 논문 쓰느라 고생 많았어 박사과정도 힘내고. 나 실험실에서 외롭다고 징징대서 자주 놀러 온 광명이, 재진 오빠, 종민이 오징어나라 또 가자. 우리 안부 아이들, 상하 상희 수지 수현 유나 지원이 다들 고마워 조만간 다시 모여서 여행계획 세우자. 동환오빠 신구오빠 미승오빠 힘내세요 1년 남았어요! 은비도 맞는 일 찾아서 열심히 하고. 혜선이, 은선이 실험실 정리 도와준 덕분에 논문 쓸 때 더 집중할 수 있었어 고마워.

미은 언니 세포 배양 처음 시작 할 때 많은 도움 주셔서 감사해요. 언니 덕분에 훨씬 수월하게 할 수 있었어요. 인준 오빠 덕분에 석사과정 시작할 때 많이 의지했고 많이 배웠어요. 모두 언급은 못했지만 모두들 감사했습니다. 2년 동안 배운 경험들 잊지 않고 어디 실험실로 가든지 잘해내겠습니다.